IEEE Journal of Microwaves

Received 5 May 2024; revised 12 June 2024; accepted 29 July 2024.

Digital Object Identifier 10.1109/JMW.2024.3438126

From RainCube to INCUS: Using Miniaturized Microwave Instruments to Analyze the Dynamics of Tropical Convection

ZIAD S. HADDAD AND OUSMANE O. SY

(Invited Paper)

Jet Propulsion Laboratory, California Institute of Technology, Pasadena, CA 91109 USA

CORRESPONDING AUTHOR: Ziad S. Haddad (e-mail: zsh@jpl.nasa.gov).

This work was supported by the National Aeronautics and Space Administration, Washington, DC, USA. This research was carried out at Jet Propulsion Laboratory, California Institute of Technology, under contract with the National Aeronautics and Space Administration ©2024 California Institute of Technology.

ABSTRACT This narrative tells the story of how NASA's INCUS (INvestigation of Convective UpdraftS) mission was conceived and designed, to identify and flesh out a scientific investigation that would be conducted using newly developed miniaturized weather radars and radiometers. Different considerations led to the conception of a new observation strategy, consisting of deploying identical replicas of the latest-technology instruments in a tight convoy in low Earth orbit. The scientific goal of this concept is to observe systematically and globally the main thermo-dynamical process in convective storms: the vertical transport of air and moisture from the surface up to the upper troposphere. How the different elements of the concept were fleshed out is recounted with specific attention to the top-level requirements placed on the microwave instruments and to their scientific justification. One of the main "morals" of the story is to highlight the need to pay close attention to the sufficiency of top-level requirements in addition to their necessity, and not to hesitate to add explicit requirements when expanding the capabilities of a heritage instrument in order to ensure that the top-level requirements are indeed sufficient as well as necessary.

INDEX TERMS Radar, severe storms, convective updrafts, millimeter-wave radiometer, Ka-band.

I. THE MINIATURIZATION REVOLUTION

The first observations from space of the vertical distribution of condensed water in clouds and precipitation were made possible by the Tropical Rainfall Measuring Mission's Precipitation Radar (TRMM-PR) launched into low-Earth-orbit in November 1997, followed by CloudSat's Cloud Profiling Radar (CPR) launched in April 2006 and the Global Precipitation Measuring Mission's Dual-frequency Precipitation Radar (GPM-DPR) launched in February 2014. The TRMM-PR and GPM-DPR use planar phased-array antennas consisting of slotted-waveguide elements. The CPR uses a fixed Cassegrain antenna. The total mass and power consumption of these instruments are given in Table 1. Although the power values appear low, they are far higher than can be obtained from cubesats. The masses are similarly incompatible with cubesat platforms.

TABLE 1 Approximate Masses and Power Consumption of Four Satellite Precipitation/Cloud Radars

Instrument	Mass	Power
TRMM-PR	465 Kg	220 W
CloudSat	230 Kg	270 W
GPM-DPR-Ku	470 Kg	440 W
GPM-DPR-Ka	330 Kg	340 W
RaInCube	5.5 Kg	22 W

Starting in 2011, in response to an internal JPL challenge to develop a radar that would be compatible with the 6U class of cubesats, Dr. Eva Peral led a team to design and build a satellite radar that would have a performance comparable to that of, say, GPM-DPR-Ka, but that would be miniaturized to fit within the size, mass and power constraints of a cubesat.

The result began to take shape in 2012, as systematic simplification and miniaturization of the radar subsystems led to an architecture where the number of components, the power consumption and the overall mass were over one order of magnitude smaller than those of existing satellite radars. One of the key elements in the total reduction in size, mass and power was to transmit (and receive) signals that use offset I/Q modulation (in-phase and quadrature) with pulse compression. Replacing the high-power short monochromatic pulses of existing satellite radars with pulse compression allowed the new design to achieve the required sensitivity with low range sidelobes (that are necessary to prevent the surface echoes from occluding the backscatter from tropospheric condensed water) without the need for high-power amplifiers and either high-voltage power supplies or large power-combining networks. The main innovation in the radar electronics was the new custom "medium-power" amplifier, fabricated with off-the-shelf GaAs solid-state pHEMT chips [1].

The other key element of the reduction in size and mass is the deployable 0.5-meter parabolic antenna reflector which, when stowed, would occupy 1.5U of the cubesat (the radar electronics occupying another 3U). That is how the RaInCube (Radar In Cubesat) design was born. In transmit mode, the power consumption of the radar would be about 22 W. Together with its antenna, the total mass of the instrument would be about 5.5 Kg. These figures suggest why RaInCube would be far less expensive to build, launch and operate than its illustrious predecessors. The reduction in cost is so stark that one can easily contemplate having several examples of RaInCube in orbit at the same time. The main disadvantages are 1) the limited power, and more ominously 2) the limited position, attitude and pointing control and accuracy. As we shall see in Section V, these limitations must be seriously considered when evaluating the ability of these miniaturized instruments to deliver observations of comparable quality with those of their larger progenitors.

In parallel with the advances in miniaturizing satellite weather radars, JPL made important strides in miniaturizing mm-wave radiometers. Using direct detection to reduce the power consumption and to remove the need for a local oscillator and mixer, the TEMPoral Experiment for Storms and Tropical systems (TEMPEST) radiometer was developed to make mechanical cross-track scans from nadir–45° to nadir+45° in several frequency bands between 90 and 190 GHz. The receivers for all channels are based on a new 35-nm InP HEMT low-noise amplifier design developed jointly by JPL and the Northrop Grumman Corporation [2].

By 2017, technology-demonstration versions of RaInCube and TEMPEST-D were ready to be deployed, and were indeed placed in orbit in June 2018 from the International Space Station. RaInCube was intended to remain operational in orbit for at least three months. It remained operational until December 2020. The data it took are described in Sy etal. [3], and are posted on JPL's Tropical Cyclone Information System portal at https://tcis.jpl.nasa.gov/data/raincube/. They include those data that were coincident and nearly simultaneous with GPM core observations. The results are visually quite impressive (see Fig. 1). Despite its coarser horizontal resolution of 8 km, RaInCube produces cross-sections through storms that show more spatial detail than the GPM radars. This is due to the decision to optimally use the time that RaInCube has along the orbit (which the GPM radars use to scan across the track) to over-sample in the along-track direction (with roughly one sample every 2 km, allowing an along-track deconvolution to refine the along-track resolution to 4 km). This oversampling allows one to apply a deconvolution albeit in the along-track dimension only, but the deconvolution results produce radar reflectivity curtains that are as plausible as those measured by GPM-DPR, with comparable detail (see Fig. 1 and the more numerous nearly-simultaneous comparisons with ground weather radar observations in Fig. 2).

Analyses of the TEMPEST-D data [4] confirms that storms can be readily identified on the two-dimensional map of any of the single-channel brightness temperatures, with the coldest temperatures corresponding to the regions of most intense convection. Comparisons with RaInCube data in 9 nearly-simultaneous coincidence events show that the correlation between the vertical integral of the dB values of the radar reflectivity factor measured by RaInCube with the brightness temperature (calculated over the coincidence segment of the orbit) is maximized for the 174 GHz and 164 GHz channels, where five out of the nine events produce correlation coefficients greater than 0.69 – with values that are comparably high for the other channels in four of these five events. Perfect correlations cannot be expected for several important reasons, including the large difference in size between the instantaneous fields of view.

One can conclude from the two technology demonstration missions that the miniaturized instruments perform comparably to their larger predecessors for a small fraction of the size, mass, power, complexity and cost. One obvious shortfall of the radar is the one-dimensional nature of its observations. This is not emphasized in the results because, in print, figures and plots cannot easily be made in more than two dimensions, but the lack of cross-track scanning places a clear limitation on the sample size as well as the amount of information that one can extract from the radar observations about the storm being observed. The option of having simultaneous radiometer observations around the track of the radar should help (and indeed does help, as discussed at the end of Section V). Another option would be to deploy several radars in different orbits so as to increase its coverage, but this would imply many launches, as many such replicas would be needed to achieve coverage that is significantly denser than that of, say, TRMM-PR. These considerations highlight the degree to which the technology preceded the science in these developments: miniaturized instruments were being designed and would soon be deployed in space, but a compelling scientific case for such deployments had not yet been articulated – indeed, how could the miniaturized instruments help generate new knowledge about variables or processes that had not yet been examined systematically?

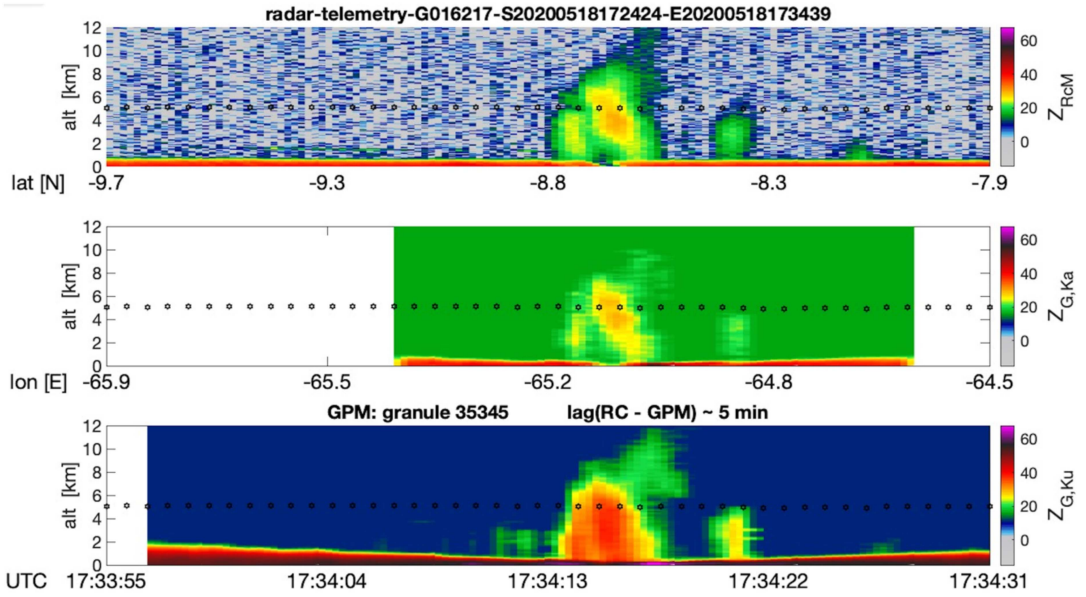

FIGURE 1. Data from the most nearly-simultaneous coincidence of RainCube with GPM radar measurements, where RainCube observed the dbZ values illustrated in the top panel about 5 minutes after the dbZ values measured by the GPM-Ka radar (middle panel) and the GPM-Ku radar (bottom panel). The 0° isotherm shown with hollow dots was derived from ECMWF reanalysis.

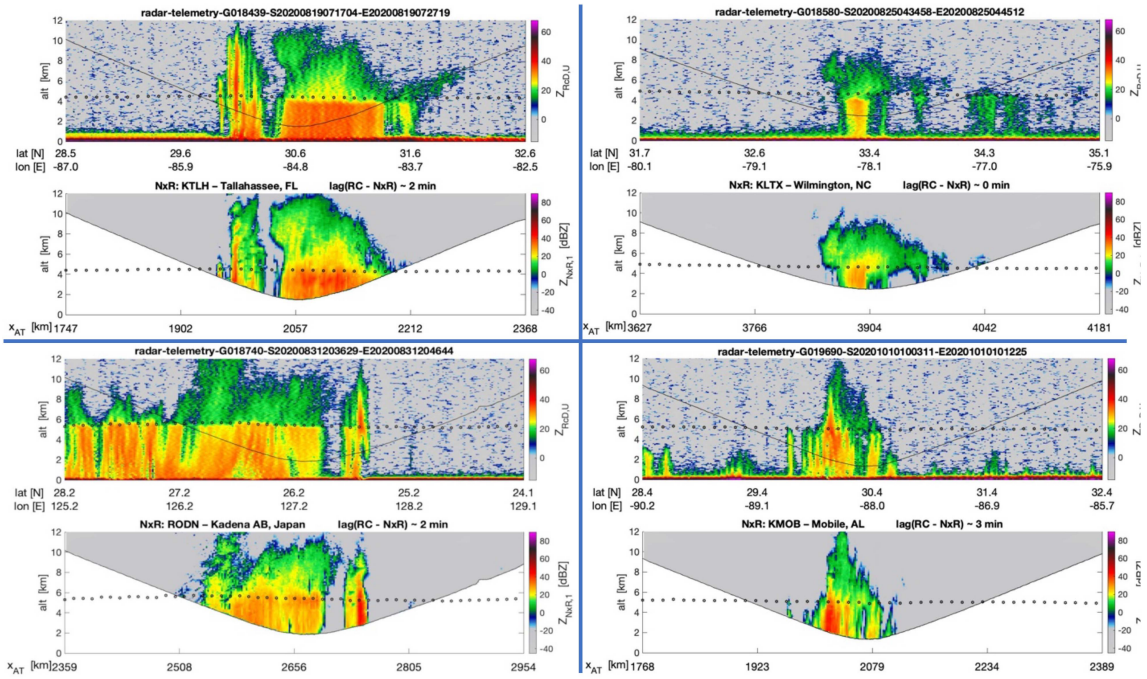

FIGURE 2. Four convective events observed nearly simultaneously by RaInCube (top panel in each quadrant) and ground radar (NOAA's WSR-88D "NEXRAD"): talahassee, FL, 19 August 2020 (top left); Wilmington, NC, 25 August 2020 (top right); Kadena AFB, Japan, 31 August 2020 (bottom left); mobile, AL, 10 October 2020. The T = 0°C-isotherm from ECMWF ERA5 is shown with a line of small circles between 4 and 6 km AMSL. Manifestly, the ground-clutter-constrained elevation scanning strategy of the ground radar severely diminishes the ground radar's ability to observe the full vertical extent of the storms.

II. SCIENCE CATCHES UP WITH THE TECHNOLOGY

An obvious application for the miniaturized radars is to deploy several replicas in different orbits, over a long-duration mission. The goal would then be to increase the coverage relative to that of a single previous-generation radar. We conducted simulations centered on an area that would encompass the continental US, say the rectangle from 130°W to 60°W and 15°N to 50°N, and tried to determine how many RaInCubes would be required to produce an observation over every 8 km pixel (the spatial resolution of RaInCube when

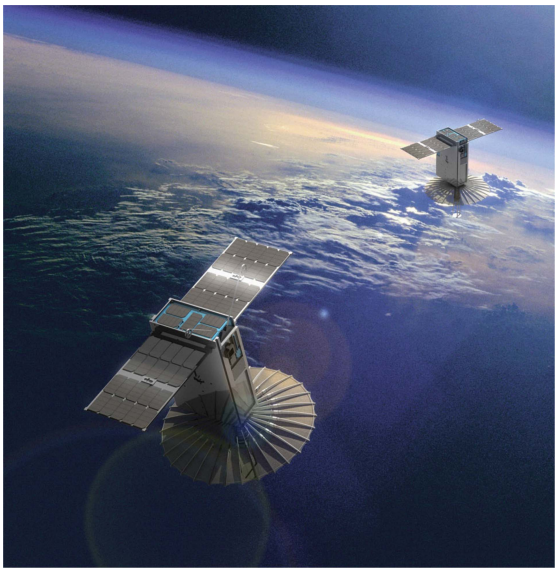

FIGURE 3. Artist's impression of a convoy of 3 RaInCubes (each the size of a shoe box) orbiting in formation.

orbiting from the same altitude as the International Space Station) at least once in any six-hour period, with no more than 3 orbital planes. The answer is at least 80 RaInCubes per plane, for a total of 240 replicas. That is much too large a number to make this concept competitive with the previous-generation scanning radars, particularly when you consider that a six-hour time window is still far too long to resolve the evolution of just about any storm. One could reduce the number of units required by increasing the size of the pixel that needs to be revisited every 6 hours – or by increasing the length of the time interval. But 8 km is already too coarse to capture convective-scale variability, and 6 hours is about as long as a window can be to sample the diurnal variability at (better than) the Nyquist rate.

A different concept would be to deploy the RaInCubes in a tight-formation convoy (Fig. 3). The idea would then be to have all the members of the convoy image the same ground pixel(s) albeit at different times. This would allow the radars to capture the evolution of radar reflectivity over the period of time that it takes the last member of the convoy to reach the current location of the leading member of the convoy. That is what ground weather radars allow one to do over their admittedly confined coverage areas: they provide information even to the casual user, showing how, in what direction and at what speed fronts move horizontally, and where vertical convective cores develop and at what spatial density. To implement this observation strategy of chronologically capturing the evolution of clouds, RaInCube would require two initial modifications:

- any member of the convoy would need to be able to complete a single cross-track $(-\theta^\circ)$-to-$(+\theta^\circ)$-to-$(-\theta^\circ)$ slewing maneuver every orbit. The angle q depends on the distance between the convoy member and the anchor of the convoy (say the one closest to the middle), and is calculated to ensure that the convoy radars all point to the same point on "the ground" (or at a fixed given altitude Above Mean Sea Level) that the anchor satellite sees at nadir. The pointing changes from one convoy member to the other because the Earth maintains a constant rotation as the convoy moves, and the change is accounted for exactly by this slewing maneuver.
- The radars need to have more than a single nadir beam, indeed they would need to scan over at least the width of three beams across track, in order to be able to identify the local horizontal movement (translation) of the storm.

The second requirement is essential for one to be able to attribute changes in the radar measurements from one convoy member to the next, to actual local changes in the condensation in the atmosphere (as opposed to mere horizontal translations of the entire storm). The goal of the convoy observations would then be to estimate the vertical component w of the motion within storms. This vertical transport is most important in storms because it is the mechanism responsible for condensing water and creating clouds: the fact that temperature is generically monotone decreasing as a function of height in the troposphere implies that, if an already saturated parcel of air is transported upward,

- it will cool, therefore the amount of water vapor it contains will exceed its new saturation pressure, therefore
- it must condense some of the vapor, creating or adding condensed water to that location in the atmosphere – where
- the change of phase from vapor to condensate releases heat,
- which forces the parcel to rise some more, cool, condense some more, release more heat, etc until the parcel literally runs out of steam. Conversely, using the very same explanation, the creation of condensed water in turn creates vertical motion (because of the accompanying heating). Thus, once advection is accounted for, the change in condensation that the radar convoy can sample is in a bijective relation with the vertical transport (see equation 2 in [5]).

As we shall see in the following section, these two modifications are necessary but not sufficient to enable the convoy concept to observe vertical transport and interpret the observations accurately. The goal is very much worth pursuing because we still do not have, today, any systematic observations of the vertical transport globally. Some ground radars and wind profilers have been used to measure w at the specific locations of these instruments on the ground and during the times that they were operated, but these samples are too sporadic to provide the global coverage needed to ensure that our ability to represent convection in today's numerical models, at all scales, is sufficiently realistic to make reliable predictions at weather (let alone climate) scales. Having accepted that the satellite radar will have a very narrow swath, it becomes that much more important to obtain ancillary information that can help characterize what portion of the storm was observed by

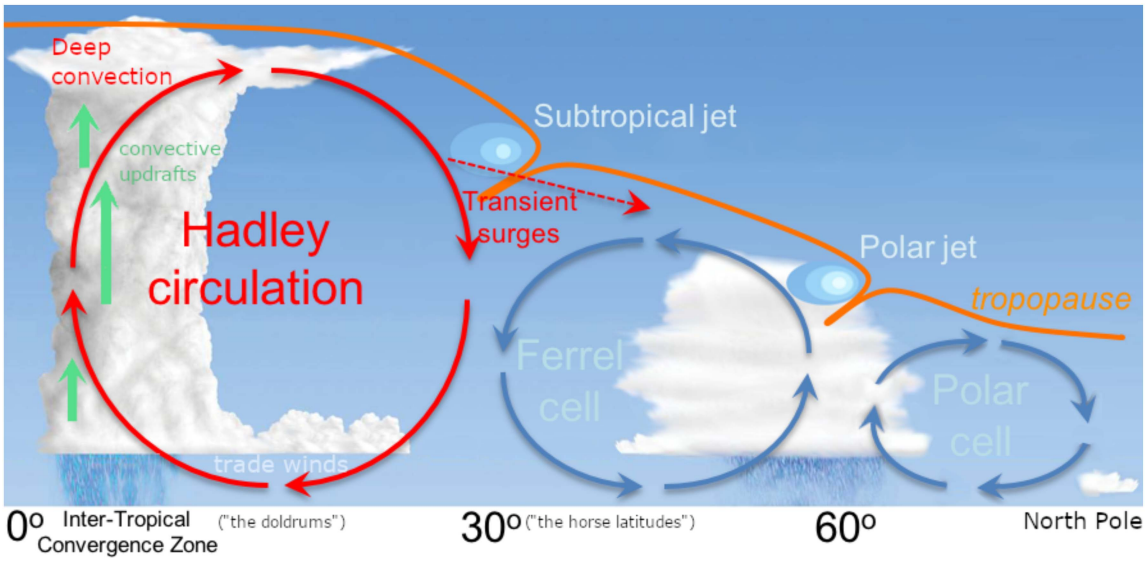

FIGURE 4. **Convection (in the "rising" branch of the Hadley circulation), especially deep convection, drives global circulation and severe weather, and is driven by the processes governing the conversion of water vapor into condensates, the accompanying latent heat producing the vertical transport.**

the radar. Were the measurements taken over the most active part of the storm or from the edges of the cloud? Providing such contextual information is what a mm-wave radiometer can do quite well. In addition to the vertically-integrated condensed water content, the radiometer measurements can be used to estimate the storm height for different low thresholds of condensed water content, as well as the top two vertical principal components of the vertical distribution of condensed water [6]. Taken together, these geophysical variables can be viewed as a proxy for convective intensity that can be derived over every ground point observed by the radiometer, i.e., typically a much larger portion (if not all) of the storm than the radar can ever observe. By locating where the value of this proxy derived directly from the radar observations fits in the radiometer-derived storm-wide distribution of this proxy, one should be able to identify what percentile a radar-derived w represents storm-wide. Indeed, a radar-observed value of 5 m/s at one location merely indicates a medium updraft at that location, but if it were accompanied by the knowledge that this represents the 5th (or 95th) percentile in the entire distribution of w over the storm, it would mean that this is an unusually intense (resp. weak) storm where most of the updrafts have speeds reaching above (resp. not exceeding) 5 m/s. For that reason, it would be highly desirable to have at least one TEMPEST-like radiometer be part of the radar convoy. Ideally, the radiometer would have an aperture that is large enough to acquire data at a spatial resolution comparable to the radar resolution or at least to the width of the radar swath (so that the nadir field of view of the radiometer would be filled with nearly simultaneous radar measurements).

So why is it important to estimate the vertical component w of the motion within storms, and how accurately could our putative convoy do that?

III. OBSERVING THE VERTICAL TRANSPORT IN CONVECTIVE STORMS

A. ROLE OF CONVECTION IN THE ATMOSPHERIC CIRCULATION

Tropical weather is driven by strong convection, with vertical transports that start at small scales and grow upscale by self-organization. The processes governing the evolution of convection, mainly the conversion of water between its three phases and the resulting heat release and subsequent transport (summarized in the previous section), are still poorly quantified. Key questions include: at what rate and with what efficiency do these conversions and vertical (and horizontal) transports occur within a convective storm? What is the functional dependence of convective transports on the environmental wind shear, buoyancy and moisture? How can we represent these processes in numerical models consistently to reproduce these transports as they evolve?

At climate scales, deep convective storms constitute the ascending branch of the Hadley circulation (Fig. 4). Deep tropical convection is the vehicle that adds mass and potential energy to the tropical upper troposphere (UT). When compared to layers at the same height in the extra-tropics, the air in the UT is of higher density, and therefore has higher potential energy. The excess tropical potential energy is essentially trapped by the inertial stability of Earth's rotation, and is "available" to be converted to kinetic energy [7]. The conversion typically results in the formation of a subtropical jet structure [8]. Thus, deep tropical convection is the vehicle that adds mass to the UT, and transport to the extra-tropics completes the energy cycle, occurring in small-scale "surges" [9] that can (and often do) spawn severe weather. Today's models still disagree in their representations of the potential energy built up by deep convection [10]. Improving the model

representation of the vertical transport associated with convection is necessary to improve our ability to forecast the effects of this transport on the global circulation.

Along with the vertical transport of air mass and energy, the vertical transport of water plays a crucial role in the evolution of the deep convective storms themselves. While surface temperature and boundary-layer moisture convergence are among the essential causes of convective initiation (CI), we do not yet have systematic observations of the dependence of CI on the relevant environmental factors, nor do we have systematic observations of the resulting transport of water, the production of condensed water mass and accompanying latent heat, and the relative fractions of condensation that remains aloft (in the anvil clouds generated by these storms) *or* sediments out locally (as surface precipitation, sometimes extreme), over the life cycle of a convective event. The evolution of this water transport, and the direct effects of microphysical processes associated with phase changes and buoyancy production, at storm lifecycle scales, are crucial in determining the very nature and evolution of the storms themselves – understanding this evolution and being able to model it substantially more realistically than our current capability is crucial if we are to improve our prediction systems at weather to climate scales.

As in the case of the transport of air to the UT, the transport of water directly affects the sensitivity of Earth's climate to forced change. Water in the atmosphere is such a strong absorber of infrared radiation, that the movement of water away from the warmer temperatures of the lower atmosphere to the colder temperatures of the upper troposphere dramatically enhances the Earth's greenhouse effect [11]. Global models of the Earth System have to make inadequately constrained assumptions about how much air and water are deposited in the upper troposphere and then what fraction of this is spread out into high clouds through the process of detrainment. Climate and hydrological sensitivities depend on the assumptions behind this pumping of water by deep convection [12]. Improving the representation of the vertical transport of water in climate models is critical to predict the climate and hydrological sensitivities [13], [14].

Numerical models simulate atmospheric circulation and the accompanying dynamical and thermodynamical processes by solving the Navier-Stokes equations, starting at a given point in time with values of all the state variables at that starting time. Being an initial value problem, the model description of the atmospheric state at any future time – including the quantitative representation of any resulting storms – are entirely determined by the initial state, though the level of detail (including spatial resolution) that is required of the initial state is not known. Thus, for convective storms, the most salient elements of the outcome i.e., the anvil cloud and the more or less abundant and/or intense surface precipitation depend directly on – and should theoretically be derivable from – this initial state, if it is known to a sufficient level of detail. The main process that creates convective storms is the vertical transport that is fueled by the latent heat of condensation of water vapor. This vertical transport is a turbulent process that cannot be sustained over areas wider than a few kilometers at a time, and in fact observations of convective plumes wider than 10 km are rare [15]. The resulting "convective updrafts" (CUs) are the building blocks of convective storms. One can define a CU as a connected volume where the condensed water content is significant (i.e., greater than a nominal minimum value, say about 0.05 g/m^3) and the vertical component of the velocity, w, is also greater than a somewhat arbitrary minimum threshold (often taken to be between 1 and 1.5 m/s, see [16]. Since CUs are the main building block of convective storms, it is reasonable to recast the relation between the initial state and the resulting anvils and surface precipitation as three separate relations: the relation between the initial state and the resulting CUs; the relation between CUs and the anvils, and the relation between the CUs and the surface precipitation. Crucially, introducing the intermediate CU in this manner will make it possible for modelers not only to verify if their model representations of convective outcomes are consistent with the initial conditions, according to observations, but also to verify if the consistence (or lack thereof) is due to their (in)accurate representation of the main process producing the outcomes, namely the vertical transport in CUs. And that is what our concept to use RaInCubes will set out to quantify: the relation between the initial state of the atmosphere and the CUs in the storm; the relation between updrafts and the resulting anvils; and the relation between updrafts and the resulting surface precipitation, in moist convection. The project will do this by generating an extensive set of systematic global observations of the vertical transport in convective updrafts. Anvil size and longevity will be obtained from geostationary IR observations of cold cloud tops. Surface rain will be sourced from the Global Precipitation Measurement mission. Environmental states will be obtained from global model re-analysis.

B. CONCEPT TO OBSERVE CONVECTIVE UPDRAFTS USING A RADAR CONVOY

To characterize a CU from radar measurements, the concept is to proceed as follows. The (vertical profiles of) radar reflectivity factors are directly sensitive to the (vertical profiles of) condensed water content Q in the troposphere. The latter evolve according to the equation

$$\frac{\partial Q}{\partial t} = \left(-u\frac{\partial Q}{\partial x} - v\frac{\partial Q}{\partial y}\right) - w\frac{\partial Q}{\partial h} + S$$

in which we identified the vertical coordinate as height h to avoid confusion with the traditional label of the radar reflectivity factor (Z). The equation states that the total change in the condensed mass at a given point in space and time (the left hand side) is due to the change due to horizontal advection (the term in parentheses on the right) and vertical "advection" i.e., convection (the second term on the right) along with the sources and sinks (combined into the scalar "S") due to the phase changes that are taking place. In saturated volumes such as convective updrafts, the source term *S* is a monotone function of w: indeed, a positive w will lift a parcel of air

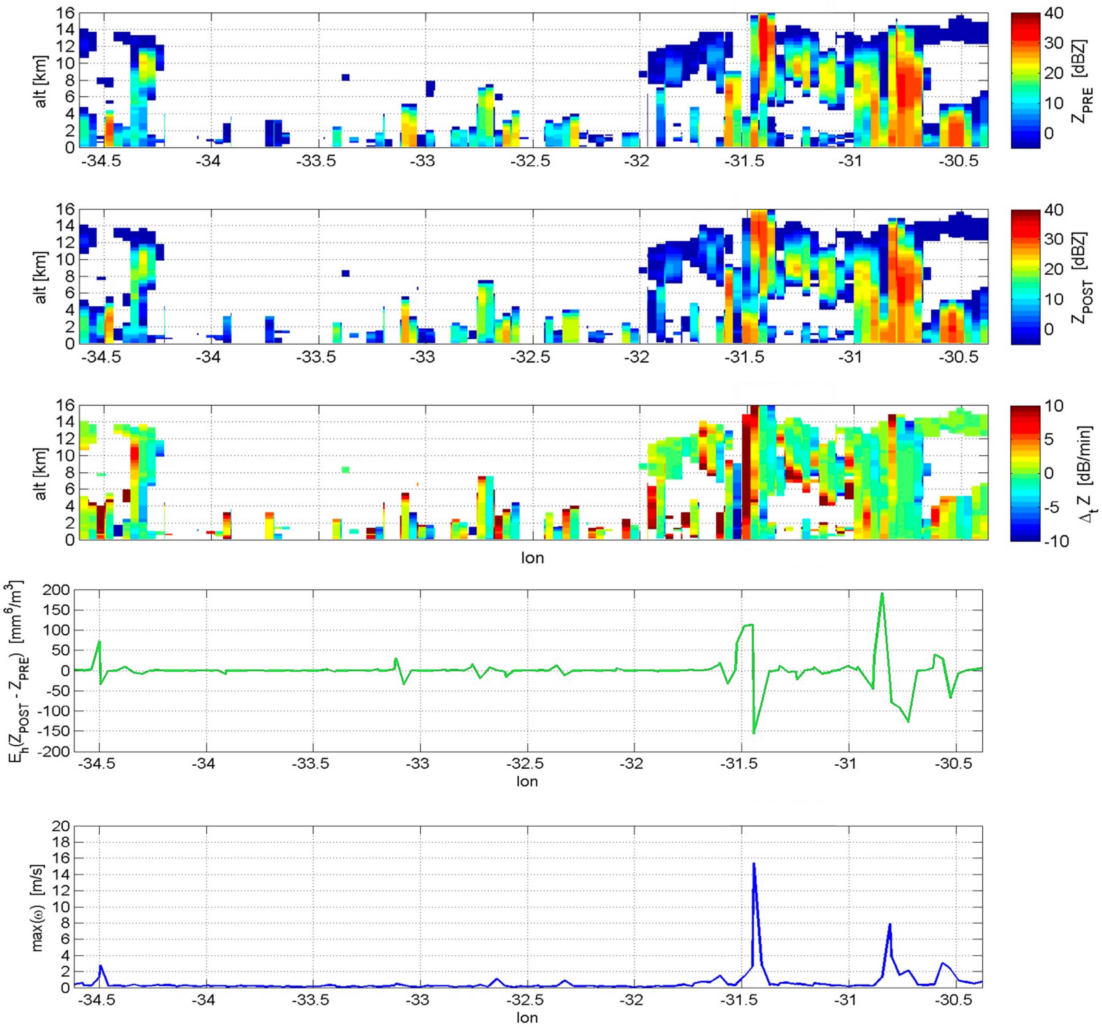

FIGURE 5. **The top two panels show the synthetic Ka-band radar reflectivity factors Z in a vertical section through a simulation of tropical storm isabel [19], at the beginning (top) and end (2nd from top) of a two minute interval. The middle panel shows the change in the radar reflectivity over the 2 minutes. The bottom two panels show the corresponding column-average time change of Z (green) and the column-maximum vertical velocity (blue) confirming that velocities greater than 2 m/s above 5000 m AMSL correspond to the largest time changes in Z.**

causing it to cool (as temperature decreases with height in the troposphere) hence forcing it to condense some of its water vapor thus increasing Q; and, conversely, positive condensation releases latent heat which in turn increases upward motion i.e., w. It was shown that a linear approximation $S = \mathrm{a}(h)$ w is quite accurate [17], so that one can proceed to solve our equation for w to obtain

$$w = \left[\frac{\partial Q}{\partial t} + \left(u\frac{\partial Q}{\partial x} + v\frac{\partial Q}{\partial y}\right)\right] / \left(\alpha\,(h) - \frac{\partial Q}{\partial h}\right)$$

Every unknown term on the right-hand side can be estimated from measured reflectivity factors if the latter are obtained over a neighborhood of one's point (whence the need to measure over a swath rather than in a curtain), including the motion vectors (u, v) which can be approximated locally the same way Atmospheric Motion Vectors are estimated by maximizing the correlation between a local image and its future translates (see Section III-B of [18], where we verify that a 15 km × 15 km window size produces estimates of the horizontal wind vector field over the storm whose correlation coefficient with the underlying truth is greater than 74%). The equation demonstrates the direct dependence of w on the spatial and temporal change of Q, to which the radars are in turn directly sensitive (see Fig. 5). This is the fundamental justification for our observation concept. However, the radar reflectivity measurements will not be sensitive to infinitesimals (whether horizontal, vertical, or temporal) – they are only sensitive to finite differences in space and time. That is why our procedure to estimate vertical profiles of w from the radar measurements will rely on constructing off-line a reference data set of local (Z, w) fields that are local in space and time, to be used to train a retrieval of the conditional mean of w given any observed Z. To construct a reference set of local solutions, one needs to produce a sufficiently representative set of small neighborhoods, say a 20 km × 20 km wide, with

solutions of the Navier-Stokes equations over, say, 2 minutes, for various combinations of initial conditions which produce at least one updraft in the volume, from which expected radar reflectivity factors at the initial and ending times could be synthesized and recorded along with the intervening values of w for any updrafts in the simulation. An efficient procedure to construct such a reference set "NIC" (of local neighborhoods in convection) is to run several regional simulations with initial states known to have produced convective storms, at high spatial resolution (on the order of 100 m) and with frequent outputs of the atmospheric state (every 30 seconds with a subset output every 10 seconds), then harvest from the outputs the 20 km $\times$ 20 km neighborhoods of convective updrafts over 2 minutes and thus assemble a reference data set. While today's models rarely succeed in representing the evolution of an entire convective storm accurately over its lifetime, the dynamical and thermodynamical equations are sufficiently well-behaved to trust a reasonably realistic model's solution in a small domain over a very short time.

To flesh out the concept and establish requirements for the radar parameters, we used a reference set NIC extracted from simulations of the atmosphere over the domain of Hurricane Isabel 24 hours before it became a hurricane, with several microphysical schemes as described in [19]. The domain of the simulations extended from 36°W to 26°W and from 6°N to 16°N and captured all scales of moist convection from isolated storms to the organized tropical depression itself.

C. RELATION TO DOPPLER APPROACHES

The notion of using a convoy of nadir-pointing reflectivity radars to estimate vertical velocity begs the question: would this be in any way preferable to using a single platform carrying a radar that is capable of measuring the line-of-sight Doppler of its targets, the cloud hydrometeors? To answer this question, one must first understand how the line-of-sight Doppler is related to the vertical wind velocity w. The relation takes the form of a convolution, of the fall speeds of the hydrometeors within the radar range resolution volume convolved with the vertical component of the wind w and, most importantly, with the projection of the platform velocity onto the line of sight. Accounting for the latter is very important because a satellite in low Earth orbit has a tangential velocity that is generically slightly greater than 7 km/s, which is three orders of magnitude greater than the terminal velocity of the generic hydrometeor. If the radar beam were infinitesimally narrow so that the line of sight is exactly orthogonal to the satellite velocity vector, the contribution of the latter to the Doppler would be 0, but in reality radar beams do have some width, and the projection of the satellite velocity onto the directions within the beam must be taken into account. One way to do this is with a receiving antenna that is physically displaced relative to the transmitting antenna – this is the Displaced Phase Center antenna concept whose application to satellite weather radars was first discussed in [24]. The added complexity that this requires in the design and size of the antenna is beyond the capability of RainCube. This added complexity is only one of the three essential differences between a Doppler approach and the new reflectivity-radar convoy concept that we developed. With Doppler, once one is reasonably assured of measuring the line-of-sight Doppler due to the hydrometeors distributed within the radar resolution volume, one would still need to distinguish the contribution of the vertical wind w from the spectrum of fall velocities of the hydrometeors, which depend on the hydrometeor sizes and habits. Various approximations can be contemplated to reduce the large number of unknowns (the hydrometeor properties) to be more comparable to the number of scalar observables (reflectivity and Doppler). Last but not least, one can only expect to retrieve an *instantaneous* w from a measured line-of-sight Doppler, without any information as to how stationary w is over the typical time scales of our models (seconds to tens of seconds). This makes the Doppler approach complementary to the reflectivity-radar-convoy concept, since the two approaches seek to measure different forms of "the vertical velocity", the former an instantaneous value, the latter an average over different short time intervals.

D. DETECTION SENSITIVITY

To set the sensitivity that would be required of our radars, we derived the distribution function of the synthesized radar reflectivity factors in columns with at least one height h where w(h) $>$ 1 m/s [19]. The results show that the 25th percentile of dbZ increases almost linearly from 5 dB at the surface to 12 dB at 4500 m Above Mean Sea Level, then remains constant at 12 dB up to 9500 m AMSL above which it decreases linearly to about 2 dB at 14000 m AMSL. Similarly, the median increases from about 12 dB at the surface to about 19 dB at 4500 m AMSL, then remains near 19 dB up to 9500 m AMSL before starting its decrease down to about 8 dB at 14000 m AMSL. These statistics justify requiring the radar sensitivity to be between 12 and 17 dB, to ensure that most of the measured reflectivity factors above the freezing level (around 4500 m in the tropics) in convective updrafts will be above the detection threshold.

E. TOLERABLE UNCERTAINTY IN THE MEASURED RADAR REFLECTIVITY FACTORS

As to the uncertainty in the measured dbZ values, the RainCube reflectivities carried an uncertainty of about 2 dB, which is quite large and potentially detrimental to our ability to make useful retrievals, so we required that the cross-calibration between a pair of radars be accurate enough to leave no more than 1 dB of uncertainty on the difference in reflectivities. This is consistent with requiring that if $\mathrm{dbZ}(t_1)$ and $\mathrm{dbZ}(t_2)$ represent the radar reflectivity factors measured at two different times from the same point in the atmosphere by two radars in our convoy, one can model them as

$$\mathrm{dbZ}\,(t_i) = \underline{\mathrm{dbZ}}_i + (7/2)^{1/2}\mathrm{X} + (1/2)^{1/2}\mathrm{Y}_i, \quad i = 1 \quad \text{or} \quad 2,$$

where $\underline{\mathrm{dbZ}}_i$ are the means, and X, Y_1 and Y_2 are independent standard normal variables, with X the common-mode error and Y_i the specific independent error in each observation.

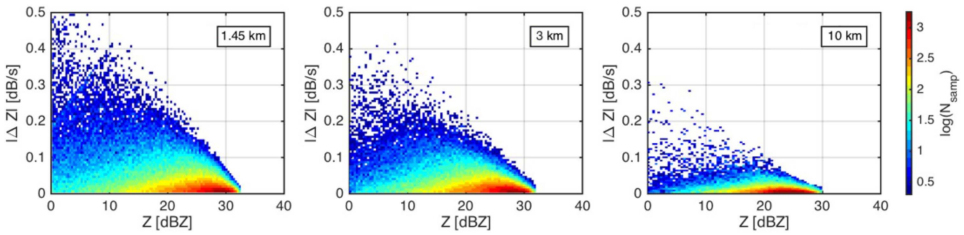

FIGURE 6. **(dbZ(t_2) – dbZ(t_1))/(t_2 – t_1) on the vertical axis, plotted versus Z(t_1) at the same point (on the horizontal axis), from our simulated CUs spatially averaged at three different scales from the original finer scale of the simulations.**

F. HORIZONTAL RESOLUTION

The required spatial resolution was determined by examining the joint distribution of our synthetic measurements i.e., the pairs (dbZ(t_1), dbZ(t_2) – dbZ(t_1)) within the simulated updrafts, derived by averaging the calculated radar reflectivities at different spatial resolutions (see Fig. 6). The reflectivities (and reflectivity differences), at the coarsest 10 km resolution that we considered (right panel in Fig. 6), still managed to capture the change in reflectivity due to the convection, but the range of values is very small and difficult to resolve given the limited ability of our measurements to distinguish these small values from random noise. At the finest resolution that we considered, 1.45 km (left panel in Fig. 6), the additional range of change values that our instruments would be able to distinguish from noise falls below our radars' detection threshold (evidently, they are not sustained over a sufficiently wide area). For a nominal 15 dB detection threshold, the proportion of cases where the change in reflectivity is greater than the nominal sensitivity threshold of 0.022 dB/sec (representing two 1db standard deviations divided by a nominal 90 second value for $t_2 - t_1$) is about 64% at the 1.45 km resolution, 54% at the 3 km resolution, 25% at the 9 km resolution, and it drops below "the majority" (i.e., 50%) when the resolution is about 3.6 km. That is the reason we set our resolution requirement (given the radar sensitivity) to be between 3 and 4 km.

G. TIME SEPARATION(S)

Since we propose to retrieve w by observing the change in the radar reflectivity between an initial and a final time, what should the separation Dt between the pair of radars be? Dt needs to be sufficiently greater than 0 to allow for the reflectivity change to grow above the measurement uncertainty in $Z(t_2) - Z(t_1)$. However, it should not be so large that the underlying w can no longer be considered stationary over that time interval. In other words, to increase detectability one would want to increase Dt, but to make sure to capture a meaningful "average w" i.e., avoid having the derivative of w make sign changes over Dt, one would want Dt to be as short as possible. In our reference set NIC at 3.6 km resolution, we found that with Dt = 4 minutes, over 50% of all convective columns have w varying by more than 150%. With Dt = 2 minutes, fewer than 20% of all convective columns have w varying by more than 80%, and that is why we chose 2 minutes as the required separation between the leading and trailing members of the convoy. And we chose Dt = 30 seconds as the required separation between the central member of the convoy and its nearest neighbor, since in our reference simulations the largest 10% of all reflectivity changes above the two-sigma threshold of 2db amounted to about 10% of the total simulated data.

H. REQUIREMENT ON THE UNCERTAINTY IN THE RETRIEVED VERTICAL SPEEDS

The considerations so far would produce a project to sample the average vertical velocity in convective updrafts at ~3.6 km horizontal resolution over intervals of 30 and 120 seconds. The main qualifier that is missing from this one-sentence summary is the required accuracy in the estimates of w. How much uncertainty can be tolerated depends on the intended use for the samples. Our analysis strategy is to

- compile observations of w in the variety of convective storms that occur in the typical wet seasons around the globe
- obtain the corresponding environmental characteristics E of the sampled storms (temperature, moisture, wind shear, and convective available potential energy or CAPE) from global reanalysis
- obtain the corresponding storm properties or outcomes O including anvil extent (from geostationary IR), condensed water volume (from the constellation of passive microwave radiometers) and surface rain (from the updated precipitation maps produced by the Global Precipitation Measurement mission)

over the total duration of the project, so that E can then be partitioned into composite classes E_i, for which the conditional distribution $p(w|E_i)$ can then be characterized, and, in turn, the conditional distributions $p(O|w)$ (and, more profitably for modelers, $p(w|O)$) can also be derived. This is a crucial element of the project: our radars will never observe an appreciable portion of any storms that they overfly, so it is only by compositing the data according to the characteristics that should, theoretically, govern the evolution of storms, that one can obtain meaningful inferences that can then be compared to the corresponding relations produced by the different models. Thus we need to ensure that the estimates of w are accurate enough to allow one to test conclusively whether the conditional distribution $p(w|E_i)$ is different from $p(w|E_j)$ if $i \neq j$. The following section summarizes how this was done.

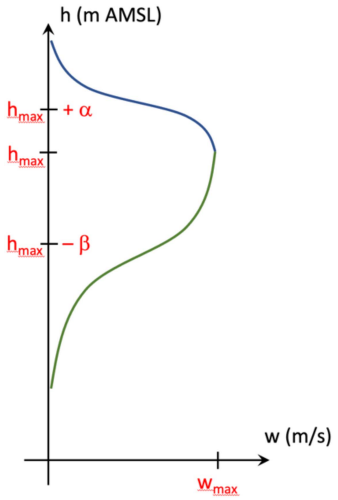

FIGURE 7. Parametric fit to w(h) in convective updrafts.

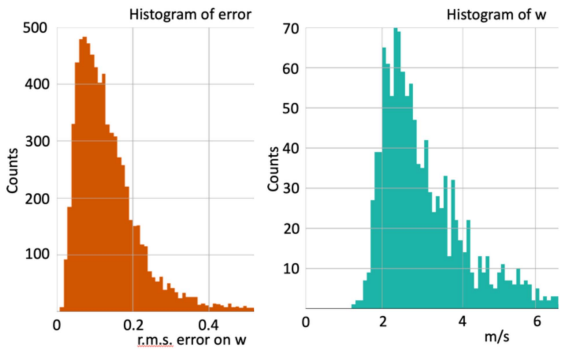

FIGURE 8. The left panel shows the column r.m.s. errors in the parametric approximation to w in our simulated convective columns. The right panel shows a histogram of w_{max} over a 250 km × 250 km generic-storm-sized octant in the domain of our simulations.

IV. MEASUREMENT UNCERTAINTY REQUIREMENT

We need to relate the uncertainty in our description of the probability distributions $p(w|E_i)$ of w to the uncertainty on the individual retrieved w. Describing $p(w|E_i)$ would be easiest if we were able to describe a vertical profile w(h) using a handful of scalar variables. To that end, we identified an analytic form using six parameters representing a "bump" extending over an interval of heights, which fits most of our simulated profiles w(h) quite well, namely

$$w(h) = \begin{cases} \dfrac{w_{\max}}{1+\frac{m-1}{m+1}\left(\frac{h-h_{\max}}{\alpha}\right)^m}, & h > h_{\max} \\ \dfrac{w_{\max}}{1+\frac{n-1}{n+1}\left(\frac{h-h_{\max}}{\beta}\right)^n}, & h < h_{\max} \end{cases}$$

where w_{max} is the column maximum value of w, h_{max} is the height at which w_{max} occurs, a is the vertical distance from h_{max} up to the height of the upper inflection point and b is the vertical distance from h_{max} down to the height of the lower inflection point (see Fig. 7), and the fifth and sixth parameters m and n control the steepness of the decrease of w(h) from its maximal value upward or downward from h. In [20], we document the latest analyses of the performance of this analytic form in approximating the vertical velocity in convective updrafts. For the purpose of describing $p(w|E_i)$, w(h) can be reduced to its 4 most essential parameters, namely (w_{max}, h_{max}, a, b), so that the probability distribution is just a scalar function of 4 scalar variables. Given our current complete lack of knowledge of the w(h) in actual CUs, knowing the conditional expectations $E\{w_{max}|E_i\}$ and $E\{h_{max}|E_i\}$ of w_{max} and h_{max} (and their conditional covariances) would go a long way to describing the differences between the different distributions.

Examining w_{max} (or h_{max}, individually), the uncertainty s^2 in our estimated sample conditional mean is the sum of two components: the actual spread of values within a given class E_i, i.e., a "true" variance s_i^2, and the spread s_E^2 due to the error in each retrieved sample value. The formula is

$$\sigma^2 = (\sigma_i^2 + \sigma_E^2)/N_i$$

where N_i is the number of samples in composite class E_i. We want to use this equation to look for the condition on s_E that will allow us to decide whether $p(w|E_i)$ is or is not different from $p(w|E_j)$. To that end, we need to guarantee that a suitable multiple of s, say 2s, is smaller than the smallest error below which two values of w_{max} cannot practically be distinguished. Since 99% of our parametric fits approximate the profile being fitted to better than 0.5 m/s (see the left panel of Fig. 8), we take this value as the tolerance margin, and we therefore require that 2s be smaller than 0.5. The value of s_i is unknown a priori, so we might as well set it to the value of the standard deviation of w_{max} over a generic storm, about 2 m/s (see the right panel of Fig. 8). To determine N_i, we need to estimate the total sample size over the duration of the putative mission. To that end, we analyzed the Tropical Rainfall Measurement Mission (TRMM) and Global Precipitation Measurement (GPM) data using different plausible definitions for "convective core" that we will use as proxies for CUs. The analysis indicates that a 39° inclined orbit with a swath width equivalent to about 3 disjoint beam diameters should fly over approximately 260,000 individual convective cores per year. Over a nominal 2-year mission, allowing for a combined duty cycle for the radars of about 80% and a data quality failure rate of about 20% (due to pointing errors etc), one can expect to sample at least 330,000 CUs. Our proposed analyses would partition this population according to storm type ("isolated", "mesoscale convective system", "tropical storm" including tropical cyclones), storm phase ("growing", "mature", "dissipating", say), and at least three classes ("low", "medium" and "high") of each of the environmental variables "temperature", "moisture", "wind shear", "CAPE". We readily concede that we will not be able to characterize the relatively rare classes, so we will assume that the population of each class of interest is no smaller than $N_i = 330000/(3 \times 3 \times 3 \times 3 \times 3 \times 3 \times 3)$. Substituting these values into our inequality $2\,[\,(s_i^2 + s_E^2)/N_i\,]^{1/2} < 0.5$ results in the inequality $4 + s_E^2 < 330000 / (3^6$

$\times$ 16), which implies the requirement $s_E < 4.9$, i.e., an r.m.s. uncertainty on the retrieved w_{max} no greater than 4.9 m/s.

For h_{max}, s_i would be 2.5 km (instead of 2 m/s for w_{max}) and the total uncertainty should be smaller than the radar-resolvable 250 m i.e., 0.25 km (instead of 0.5 m/s for w_{max}) so that the condition on the allowable error is $6.25 + s_E{}^2 < 330000 / (3^6 \times 16 \times 4)$, implying the requirement $s_E < 0.9$, i.e., an r.m.s. uncertainty on the retrieved h_{max} no greater than 900 m.

It is important to emphasize that we do not currently have very reliable detectors of convective updrafts. The figure of 330 000 was obtained using different criteria based on the instantaneous radar reflectivity measurements obtained by the GPM radars, but these are definitely not exact criteria in the sense that they have not been established to be either necessary or sufficient for the presence of a convective updraft. That is why we chose to keep the analysis very conservative and avoided accounting for the significant correlations known to exist between the four environmental variables (which would have increased the sample size in each composite class). Nevertheless, two similar analyses were conducted recently, the first [21] being a pixel-by-pixel analysis relating the environmental variable values in a grid column to the microwave-derived ice-water-path and surface rainrate in the same column in the GPM observations, and the other [22] being an "instantaneous precipitation feature"-specific analysis relating the environmental variables in the contiguous pixels making up the feature, on one hand, to the microwave-derived precipitation characteristics of the feature, "feature" being as defined in [23]. Both analyses indicate that the top two principal components of the environmental state are sufficient to distinguish between the different convective outcomes. This implies that we should be able to replace the factor "3 $\times$ 3 $\times$ 3 $\times$ 3" by "9x9" (using a partitioning of each of the top two principal components of E_i into 9 contiguous segments), which does seem to be wastefully over-precise, or replace the ratio 330000//(3 $\times$ 3 $\times$ 3 $\times$ 3 $\times$ 3 $\times$ 3) by the slightly larger 36667/(3 $\times$ 3 $\times$ 3 $\times$ 3) which corresponds to assuming that we would lose, by some catastrophe, 89% of all the radar observations (to end up with only three months' worth of data) and then partitioning according to the terciles of the top two principal components.

The last but perhaps most important top-level requirement concerns the pointing accuracy of the three radars to ensure that when looking at the same resolution element, the three fields of view do indeed capture essentially the same area. This requirement was derived by applying our prototype retrieval algorithm to inputs that consisted of the simulated radar reflectivities calculated with deliberate displacements between the initial and final fields of view. This exercise revealed that when the overlap is decreased from 100% to 82%, the r.m.s. error on the retrieved w increases by about 10%. To limit the error increase to be no greater than this nominal 10%, we required that the overlap be no less than 82%. From an altitude of about 500 km, this implies that the difference in the pointing angles of the two radars should not exceed 0.1 degree, which can be guaranteed if the 2-sigma pointing uncertainty on any one radar is kept below 0.05 degree, i.e., the r.m.s. uncertainty should be no greater than 0.025 degree.

V. INVESTIGATION OF CONVECTIVE UPDRAFTS–(INCUS)

The project was formulated as summarized in the previous section – a convoy of three vertically profiling Ka radars each scanning a swath about 15 km wide with separations of 30 seconds between the leading and middle radar and 90 seconds between the middle and trailing radar, and the proposal was submitted in March 2021 to NASA's third "Earth Ventures – Mission" solicitation. Seven months later, NASA officially selected the project to be the agency's third EV-M mission and named it Investigation of Convective Updrafts – INCUS. On the science side, the Principal Investigator, Colorado State University's Prof. Sue van den Heever started on

- designing and organizing the production of an extensive set of high-resolution simulations that would yield a sufficiently representative set of simulated local updrafts on which the estimation algorithms could be based,
- verifying that the analysis strategy would indeed be practically feasible without requiring prohibitively fine detail in the data that would come from the program of record,
- fleshing out and coordinating all the elements of the verification and validation strategy

On the engineering side, the project manager, JPL's Dr. Yunjin Kim, focused on organizing and leading

- the review of the formal top-level requirements for consistency and feasibility,
- the derivation of the lower-level requirements,
- defining the development of the non-heritage elements of the design including most notably a) the deployable antenna reflector (which essentially tripled in size relative to RaInCube's), b) the multiple antenna feeds that are needed to produce the swath (and verify that they will produce beam patterns that are not so different as to affect the observation strategy), c) the switch that controls the flow of the transmit and receive signals to and from the antenna,
- the process of securing parts amid the industry-wide scarcity and constraints resulting from the covid-19 pandemic.

The most serious and possibly show-stopping issue arose soon after the project was selected, as we were informed that the antenna could simply not deliver the very low uncertainty of 0.025° on the pointing. The counter-offer was to loosen the requirement to 0.25°, which would be reasonably easy to meet. Would an uncertainty of 0.25° instead of 0.025° be acceptable?!

The answer was of course "no", not if we wanted the nadir beam of radar 1 to observe the same spot (to within 82% overlap) as the nadir beam of radar 2, and the next beam to port of radar 1's nadir beam to observe the same spot as the next beam to port of radar 2's nadir beam, etc. We scrambled to devise a solution before the project manager had a chance to start foreclosure proceedings on the project.

The design, as proposed, would give each radar antenna a 1.6 m reflector illuminated by 5 feeds each having a 0.35° beamwidth i.e., producing a 3.1 km-wide field-of-view from a nominal altitude of 500 km AMSL. With a slight overlap between contiguous beams, this design produces a 15 km cross-track swath which we had shown was sufficient to estimate and account for horizontal advection [19]. Instead of "slightly overlapped contiguous beams", consider what would happen if we had highly overlapped beams: starting with two perfectly overlaid 3.6 km-wide fields-of-view, start moving one of them laterally so that the overlap decreases; when the distance between the beam centers reaches 0.16 diameters i.e., about 0.6 km, the overlap area decreases from 100% to 82%; this implies that if we move the next beam center further and place it at twice this distance, i.e., 1.2 km, we guarantee that any 3.6 km-wide disk whose center lies between the centers of our first and second beams *must* overlap one or the other beam by at least 82% … We thus had a solution to our pointing predicament, namely design the feeds so that contiguous beam centers are (1.2 km i.e.,) 0.135° apart. We were greatly helped by the fact that the antenna design could accommodate 7 feeds (instead of the original 5), which, if they are arranged so that they overlap pairwise by 0.135°, would produce a swath of about $1.8 + 6 \times 1.2 + 1.8 = 10.8$ km. And we duly verified using simulations that, with such a feed array, a correlation-maximizing search among the centers of a 7×7-beam domain does indeed succeed in identifying the translation to achieve 82% beam overlap. We also verified on several subdomains extracted from our simulations that the 10.8 km swath suffices to estimate the advection using the original consecutive-image-correlation approach.

The beam-overlap approach serendipitously uncovered – and pointed to a solution for – a problem which we had failed to recognize in our redesign of the antenna to create a swath, namely the fact that our beams cannot have identical antenna patterns. This is unavoidable when all but one of the feeds are (necessarily) offset from the optimal location. The solution was to use the highly overlapped sampling with the accurate expression for every beam pattern to deconvolve the observations onto a regular grid. We verified that this results in re-sampled radar reflectivities whose errors are well below the required accuracy as summarized in III.D above.

Finally, work is on-going to establish a rigorous relationship between the radar observations of any storm updrafts that happen to fall within its swath, on one hand, and the storm-wide distribution of updrafts at that same instant in time. The former represent a very small sampling of the latter, because of the very limited radar swath, but the vertical integral of condensed water (the so-called "ice water path", IWP) can serve as a reasonable proxy, since it is correlated with w (updrafts inevitably correspond to local maxima of IWP) albeit in a specific manner that varies from storm to storm depending also on the phase of the storm. Most simply, the problem can be formulated as one of determining the storm-wide conditional mean and standard deviation of w conditioned on the radiometer-observed IWP, say for simplicity finding linear regressions $E\{w|IWP\} = a\ IWP + b$ and $E\{s|IWP\} = c\ IWP + d$, and determining a, b, c and d given the radar-observed w and the corresponding radar-derived IPW in those CUs. This formulation suggests that the radars need to have observed at least 4 CUs in order to determine the coefficients in these approximate relations deterministically. However, one can reparametrize these relations and show that the ratio a/c can be directly derived from the values of the 3 remaining parameters so that, for a deterministic solution, the radar needs to have observed at least 3 CUs – and in fact a single CU could be useful if one were to introduce a regularizing term requiring the parameters to remain not too far from "background" values for the w–IWP histogram relations which one could obtain, from example, from a large number of convection-permitting simulations. In either approach, the larger the number of radar observations, the less uncertainty there would be in the resulting histogram relations. The real problem is slightly more complicated due to the fact that w is not a single scalar – but it can be characterized by a handful of scalars –, and one must then capitalize on the fact that the radiometer information is also not a single scalar and requires three or four principal components to capture most of its information content. The approach to determine the relation between the radiometer-derived histogram of IWP and the radar-resolution histogram of w remains as it is summarized above if one replaces w and IWP by their respective principal components.

The project, now officially a NASA Mission (having passed Key Decision Point C), is currently in "Phase C" through March 2025, when the integration- and-testing phase D starts with a launch date currently expected toward the end of the summer of 2026.

VI. BEYOND INCUS

One of the most important and potentially rewarding areas of research and development to improve the capability of our miniaturized radars and radiometers concerns the antenna. In the case of the radar, having the ability to scan a wider swath so as to capture a significant portion of – if not the entire – storm without sacrificing spatial resolution would be revolutionary. In the case of the radiometer, having a larger aperture so as to achieve a finer spatial resolution e.g., comparable to that of the radar would also be revolutionary.

Another area where further research could produce breakthroughs is in combining the storm-wide coarse-3d-resolution information obtainable from the radiometer with the very-narrow-swath fine-3d-resolution information obtainable from the radar to maximize the increase in our understanding – of the model, the analysis, and the forecast. The discussion at the end of the previous section is a step in that direction, but a systematic approach that reconciles the level of three-dimensional detail (of the radar observations) with the spatial organization of the information and the coverage (of the radiometer observations) would go a long way in optimizing the yield of the simultaneous nearly-coincident measurements of both instruments, leading to a more complementary use of the

radiometer to "reveal the context" of the radar observations and vice versa.

Last but not least, the problem of mitigating the limitations of the small platforms that accommodate the miniaturized instruments deserves closer attention to allow these instruments to deliver the full extent of the improvements that they promise.

ACKNOWLEDGMENT

Government sponsorship acknowledged. This research was carried out at Jet Propulsion Laboratory, California Institute of Technology, under contract with the National Aeronautics and Space Administration. ©2024 California Institute of Technology.

REFERENCES

[1] E. Peral et al., "Radar technologies for earth remote sensing from CubeSat platforms," *Proc. IEEE*, vol. 106, no. 3, pp. 404–418, Mar. 2018, doi: 10.1109/JPROC.2018.2793179.

[2] S. Padmanabhan et al., "Radiometer payload for the temporal experiment for storms and tropical systems technology demonstration mission," in *Proc. IEEE Int. Geosci. Remote Sens. Symp.*, Fort Worth, TX, USA, 2017, pp. 1213–1215, doi: 10.1109/IGARSS.2017.8127176.

[3] O. O. Sy et al., "Scientific products from the first radar in a CubeSat (RaInCube): Deconvolution, cross-validation, and retrievals," *IEEE Trans. Geosci. Remote Sens.*, vol. 60, 2022, Art. no. 1000320, doi: 10.1109/TGRS.2021.3073990.

[4] C. Radhakrishnan et al., "Cross validation of TEMPEST-D and RainCube observations over precipitation systems," *IEEE J. Sel. Topics Appl. Earth Observ. Remote Sens.*, vol. 15, pp. 7826–7838, 2022, doi: 10.1109/JSTARS.2022.3199402.

[5] S. Prasanth et al., "Quantifying the vertical transport in convective storms using time sequences of radar reflectivity observations," *J. Geophys. Res., Atmospheres*, vol. 128, no. 10, 2023, Art. no. e2022JD037701, doi: 10.1029/2022JD037701.

[6] Z. S. Haddad, R. C. Sawaya, S. Kacimi, O. O. Sy, F. Joseph Turk, and J. Steward, "Interpreting mm-wave radiances over tropical convective clouds," *J. Geophys. Res., Atmospheres*, vol. 122, pp. 1650–1654, 2017, doi: 10.1002/2016JD025923.

[7] E. N. Lorenz, "Available potential energy and the maintenance of the general circulation," *Tellus*, vol. 7, pp. 157–167, 1955.

[8] T. N. Krishnamurti, "On the role of the subtropical jet stream of winter in the atmospheric general circulation," *J. Meteorol.*, vol. 18, pp. 657–670, 1961.

[9] J. R. Mecikalski and G. J. Tripoli, "Inertial available kinetic energy and the dynamics of tropical plume formation," *Monthly Weather Rev.*, vol. 126, pp. 2200–2216, 1998, doi: 10.1175/1520-0493(1998)126<2200:IAKEAT>2.0.CO;2.

[10] W. C. D. Rooy et al., "Entrainment and detrainment in cumulus convection: An overview," *Quart. J. Roy. Meteorological Soc.*, vol. 139, pp. 1–19, 2013, doi: 10.1002/qj.1959.

[11] G. L. Stephens and B. H. Kahn, "The super greenhouse effect in a changing climate," *J. Climate*, vol. 29, no. 15, pp. 5469–5482, 2016, doi: 10.1175/JCLI-D-15-0234.1.

[12] M. Zhao, "An investigation of the connections among convection, clouds, and climate sensitivity in a global climate model," *J. Climate*, vol. 27, pp. 1845–1862, 2014.

[13] T. P. Lane and M. W. Moncrieff, "Characterization of momentum transport associated with organized moist convection and gravity waves," *J. Atmospheric Sci.*, vol. 67, pp. 3208–3225, 2010.

[14] NASA, *Workshop Report on Scientific Challenges and Opportunities in the NASA Weather Focus Area*. X. Zeng et al., Ed., 2015. [Online]. Available: https://smd-cms.nasa.gov/wpcontent/uploads/2023/05/Weather_Focus_Area_Workshop_Report_2015_0.pdf

[15] J. P. Mulholland, J. M. Peters, and H. Morrison, "How does LCL height influence deep convective updraft width?," *Geophys. Res. Lett.*, vol. 48, no. 13, 2021, Art. no. e2021GL093316, doi: 10.1029/2021GL093316.

[16] P. A. Lemone and E. J. Zipser, "Cumulonimbus vertical velocity events in GATE. Part 1: Diameter, intensity and mass flux," *J. Atmospheric Sci.*, vol. 37, pp. 2444–2457, 1980.

[17] L. D. Grant et al., "A linear relationship between vertical velocity and condensation processes in deep convection," *J. Atmospheric Sci.*, vol. 79, no. 2, pp. 449–466, 2022, doi: 10.1175/JAS-D-21-0035.1.

[18] Z. S. Haddad, O. O. Sy, S. Hristova-Veleva, and G. L. Stephens, "Derived observations from frequently sampled microwave measurements of precipitation. Part I: Relation to atmospheric dynamics," *IEEE Trans. Geosci. Remote Sens.*, vol. 55, no. 6, pp. 3441–3453, Jun. 2017, doi: 10.1109/TGRS.2017.2671598.

[19] O. O. Sy, Z. S. Haddad, G. L. Stephens, and S. Hristova-Veleva, "Derived observations from frequently sampled microwave measurements of precipitation. Part II: Sensitivity to atmospheric variables and instrument parameters," *IEEE Trans. Geosci. Remote Sens.*, vol. 55, no. 5, pp. 2898–2912, May 2017, doi: 10.1109/TGRS.2017.2656061.

[20] S. Prasanth, Z. S. Haddad, S. C. van den Heever, P. Marinescu, S. Freeman, and D. Posselt, "Parametric representation of convective updrafts and identification of the modes governing their temporal evolution," In preparation, 2024.

[21] J.-F. Rysman, C. Cloud, and S. Dafis, "Global monitoring of deep convection using passive microwave observations," *Atmospheric Res.*, vol. 247, 2021, Art. no. 105244, doi: 10.1016/j.atmosres.2020.105244.

[22] P. Marinescu et al., "Relating the convective properties of instantaneous precipitation features observed by GPM to their environmental state," In preparation, 2024.

[23] C. Liu, E. J. Zipser, D. J. cecil, S. W. Nesbitt, and S. Sherwood, "A cloud and precipitation feature database from nine years of TRMM observations," *J. Appl. Meteorol. Climatol.*, vol. 47, no. 10, pp. 2712–2728, 2008, doi: 10.1175/2008JAMC1890.1.

[24] S. L. Durden, R. M. Beauchamp, S. Graniello, V. Venkatessh, and S. Tanelli, "DPCA-based Doppler radar measurements from space: Effect of system errors on velocity estimation performance," *J. Atmospheric Ocean. Technol.*, vol. 40, no. 7, pp. 855–864, 2023, doi: 10.1175/JTECH-D-22-0048.1.

ZIAD S. HADDAD received the Ph.D. degree in mathematics from the Massachusetts Institute of Technology (MIT), Cambridge, MA, USA, in 1983.

He held several teaching and research positions with the University of California, Berkeley, Berkeley, CA, USA, MIT and the University of California, San Diego, La Jolla, CA, where he taught mathematics and conducted research on wave propagation in random media, before joining the technical staff with the Jet Propulsion Laboratory, California Institute of Technology, Pasadena, CA, in 1991. Since then, he has analyzed radar detection and tracking problems, modeled acoustic and electromagnetic wave propagation in complex media, developed nonlinear filtering and estimation techniques to retrieve geophysical data from radar observations.

OUSMANE O. SY received the M.Sc. degree in aerospace engineering from the École Nationale de l'Aviation Civile (ENAC), Toulouse, France, in 2003, the M.Res. degree in electromagnetics and optical telecommunications from Paul Sabatier University (UPS, DEA), Toulouse, in 2003, and the Ph.D. degree in electromagnetics from the Eindhoven University of Technology (TU/e), Eindhoven, The Netherlands, in 2009. In 2009, he joined the Jet Propulsion Laboratory (JPL).

His research interests include spaceborne profiling radars, Doppler radars, and stochastic uncertainty quantification.